

Discovery of a new bona fide luminous blue variable in Norma^{*}

V. V. Gvaramadze,^{1,2,3,†} A. Y. Kniazev,^{4,5,1} and L. N. Berdnikov^{1,6,3}

¹*Sternberg Astronomical Institute, Lomonosov Moscow State University, Universitetskij Pr. 13, Moscow 119992, Russia*

²*Space Research Institute, Russian Academy of Sciences, Profsoyuznaya 84/32, 117997 Moscow, Russia*

³*Isaac Newton Institute of Chile, Moscow Branch, Universitetskij Pr. 13, Moscow 119992, Russia*

⁴*South African Astronomical Observatory, PO Box 9, 7935 Observatory, Cape Town, South Africa*

⁵*Southern African Large Telescope Foundation, PO Box 9, 7935 Observatory, Cape Town, South Africa*

⁶*Astronomy and Astrophysics Research division, Entoto Observatory and Research Center, P.O.Box 8412, Addis Ababa, Ethiopia*

Accepted 2015 September 29. Received 2015 September 29; in original form 2015 August 11

ABSTRACT

We report the results of optical spectroscopy of the candidate evolved massive star MN44 revealed via detection of a circular shell with the *Spitzer Space Telescope*. First spectra taken in 2009 May–June showed the Balmer lines in emission as well as numerous emission lines of iron, which is typical of luminous blue variables (LBVs) near the visual maximum. New observations carried out in 2015 May–September detected significant changes in the spectrum, indicating that the star became hotter. We found that these changes are accompanied by significant brightness variability of MN44. In particular, the I_c -band brightness decreased by ≈ 1.6 mag during the last six years and after reaching its minimum in 2015 June has started to increase. Using archival data, we also found that the I_c -band brightness increased by ≈ 3 mag in ≈ 30 yr preceding our observations. MN44 therefore represents the seventeenth known example of the Galactic bona fide LBVs. We detected a nitrogen-rich knot to the northwest of the star, which might represent an interstellar cloudlet interacting with the circumstellar shell. We discuss a possible association between MN44 and the *INTEGRAL* transient source of hard X-ray emission IGR J16327–4940, implying that MN44 might be either a colliding-wind binary or a high-mass X-ray binary.

Key words: line: identification – circumstellar matter – stars: emission-line, Be – stars: evolution – stars: individual: EM*VRMF 55 – stars: massive

1 INTRODUCTION

Some massive stars evolve through the so-called luminous blue variable (LBV) phase in the course of their life (Conti 1984). During this phase, they experience episodes of enhanced (sometimes eruptive) mass loss, which is manifested in appearance of strong emission lines in their spectra. These episodes, lasting from years to decades and more, are accompanied by major brightness and spectral variability – the defining characteristics of the very rare class of objects called LBV stars (Humphreys & Davidson 1994). Recent searches for new members of this class though detection of their circumstellar nebulae (a common attribute of the LBVs; Clark, Larionov & Arkharov 2005; Kniazev, Gvaramadze & Berdnikov 2015) resulted in discovery of several dozens of compact mid-infrared nebulae of various morphology (Gvaramadze, Kniazev & Fabrika 2010a), whose central stars exhibit rich emission spectra, typical of bona fide LBVs (Gvaramadze et al. 2010a,b, 2012a; Wachter et al. 2010, 2011; Stringfellow et al. 2012a,b; Flagey et al. 2014). These discoveries nearly doubled the known population of Galactic candidate LBVs (cLBVs). To prove their LBV status a significant spectral and photometric variability has to be detected. Disclosure of new bona fide LBVs is of high importance for understanding the nature of their variability and the role of the LBV phase in the stellar evolution.

In this paper, we present recent results of our ongoing spectroscopic and photometric monitoring of the newly identified cLBVs, aimed to detect changes in their spectra and brightness. Our monitoring campaign, started in 2009, has already resulted in discovery of two new Galactic bona fide LBVs – Wray 16-137 (Gvaramadze et al. 2014) and WS1 (Kniazev et al. 2015). Here, we report the discovery of the

^{*} Based on observations made with the Southern African Large Telescope (SALT) under the program 2015-1-SCI-017 (PI: A.Y. Kniazev).

[†] E-mail: vgvaram@mx.iki.rssi.ru (VVG)

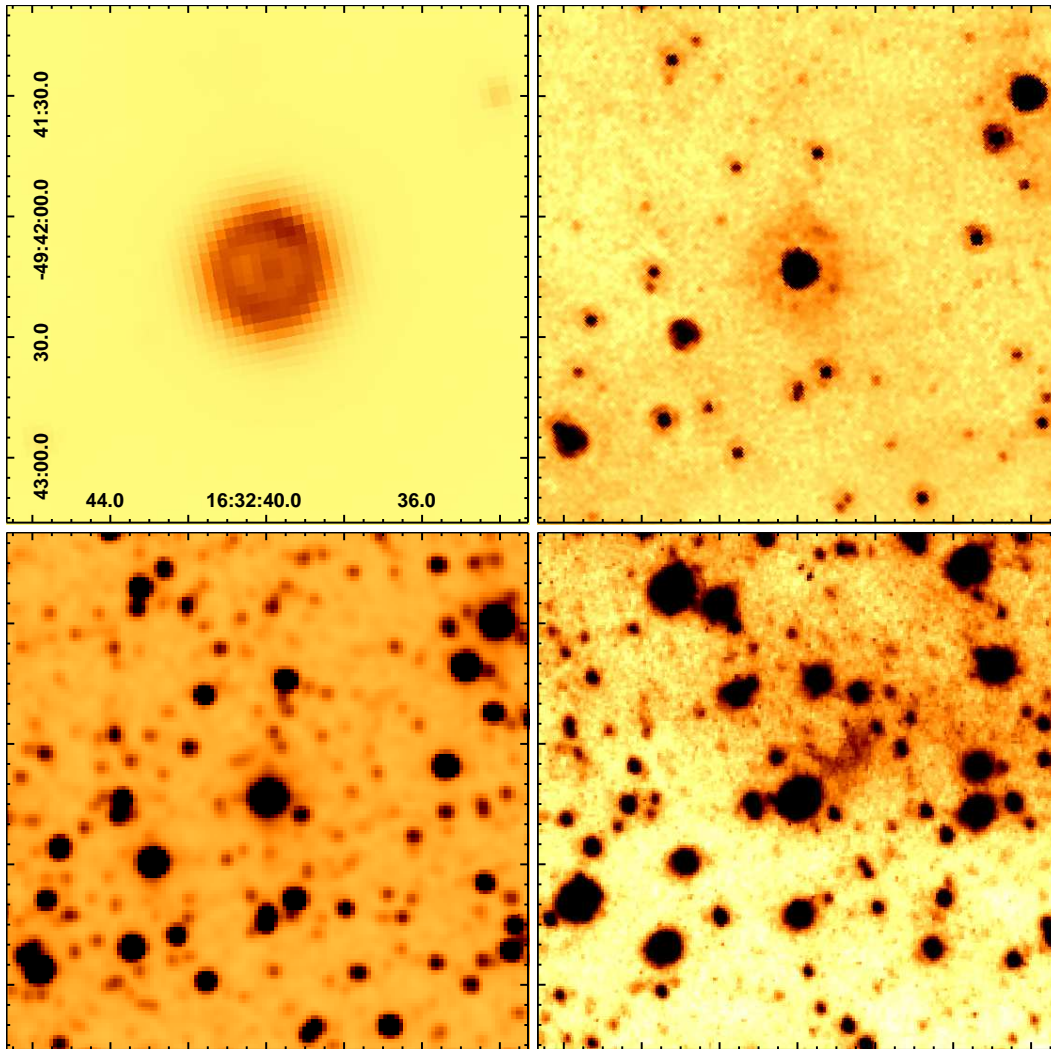


Figure 1. From left to right, and from top to bottom: *Spitzer* MIPS 24 μm and IRAC 8 μm , 2MASS K_s -band and SHS $H\alpha$ + $[N\text{ II}]$ images of the region containing the circular shell MN44 and its central star (the scale of the images is the same). The coordinates are in units of RA (J2000) and Dec. (J2000) on the horizontal and vertical scales, respectively.

third Galactic bona fide LBV – MN44, whose LBV candidacy was suggested by the presence of a circular shell around it (Gvaramadze et al. 2010a). In Section 2, we present for the first time the images of the shell and its central star at several wavelengths, and review the existing data on the central star. In Section 3 we describe our spectroscopic and photometric observations. The results and implications are discussed in Section 4. We summarize and conclude in Section 5.

2 CIRCULAR SHELL MN44 AND ITS CENTRAL STAR

The circular shell MN44¹ is located in the Norma constellation and it is one of many dozens of mid-infrared com-

pact nebulae discovered by Gvaramadze et al. (2010a) in the 24 μm archival data of the *Spitzer Space Telescope* obtained with the Multiband Imaging Photometer for *Spitzer* (MIPS; Rieke et al. 2004) within the framework of the 24 and 70 Micron Survey of the Inner Galactic Disk with MIPS (Carey et al. 2009). In the MIPS 24 μm image MN44 appears as a limb-brightened circular shell of radius and thickness of ≈ 15 and 6 arcsec, respectively, centred on a point-like source (see Fig. 1). The central point source (star) is also visible in all (3.6, 4.5, 5.8 and 8.0 μm) images obtained with the *Spitzer* Infrared Array Camera (IRAC; Fazio et al. 2004) within the Galactic Legacy Infrared Mid-Plane Survey Extraordinaire (Benjamin et al. 2003), as well as in all (J , H , K_s) Two-Micron All Sky Survey (2MASS) images (Skrutskie et al., 2006). The 2MASS coordinates of this star are: RA(J2000)=16^h32^m39^s.95, Dec.(J2000)=-49°42′13″.8 and $l=335^\circ 0635$, $b=-1^\circ 1557$. In the following, we will use the name MN44 only for the central star.

Fig. 1 shows that the nebula could also be discerned in the IRAC 8 μm image and that there is the gleam of

¹ In the Set of Identifications, Measurements and Bibliography for Astronomical Data (SIMBAD) data base this shell is named [GKF2010] MN44.

Table 1. Journal of the observations.

Spectrograph	Date	Exposure (min)	Spectral scale (\AA pixel^{-1})	Spatial scale (arcsec pixel $^{-1}$)	Slit/Seeing (arcsec)	Spectral range (\AA)
Cassegrain (SAAO 1.9-m)	2009 May 31	3×15	2.3	1.4	2.0×180/1.0	4200–8100
Cassegrain (SAAO 1.9-m)	2009 June 2	3×20	2.3	1.4	2.0×180/1.3	4200–8100
RSS (SALT)	2015 May 6	1.5+15	0.97	0.51	1.25×480/1.0	4200–7300
RSS (SALT)	2015 June 14	1+20	0.97	0.25	1.25×480/2.5	4350–7450
RSS (SALT)	2015 August 2	1+25	0.97	0.25	1.25×480/2.0	4200–7300
RSS (SALT)	2015 September 8	1+25	0.97	0.25	1.25×480/1.4	4200–7300

emission around the star in the $H\alpha$ + $[N\text{ II}]$ image obtained in the framework of the SuperCOSMOS H-alpha Survey (SHS; Parker et al. 2005). The SHS image also shows a knot of enhanced emission to the northwest of the star. This knot partly delineates the diffuse emission around the star and then curves in the northeast direction. Comparison of the 24 and $8\mu\text{m}$ images with the SHS one shows that the shell is brighter at the place of possible contact with the knot, which might be caused by interaction of the shell with a density inhomogeneity in the ambient medium. The nature of the optical emission around MN44 is further discussed in Section 4.2.

MN44 was identified as an emission-line star by Vega et al. (1980), who searched for $H\alpha$ -emission objects using objective-prism spectra. In the SIMBAD data base this star is named EM* VRMF 55. According to Vega et al. (1980), in 1974 the V -band magnitude of MN44 was fainter than 15.58. MN44 is located within the error circle of radius of 4.5 arcmin of the *INTEGRAL* transient source of hard X-ray emission IGR J16327–4940 (Bird et al. 2010). Masetti et al. (2010) obtained an optical spectrum of MN44 on 2009 August 10 using the 1.9-m telescope of the South African Astronomical Observatory (SAAO) (see their fig. 7) and broadly classified it as an OB star due to the strength of its $H\alpha$ emission line, “which is much larger than the typical values seen in blue supergiants”. These authors tentatively associated MN44 with IGR J16327–4940 and classified this X-ray source as a high-mass X-ray binary (HMXB) because of its “overall early-type star spectral appearance, which is typical of this class of objects”. Possible implications of this association are discussed in Section 4.4.

3 OBSERVATIONS

First spectra of MN44 were obtained with the SAAO 1.9-m telescope on 2009 May 31 and June 2. The observations were performed with the Cassegrain spectrograph using a slit of 3 arcmin \times 2 arcsec and grating with 300 lines mm^{-1} . This spectral setup covered a wavelength range of ≈ 4200 –8100 \AA with a reciprocal dispersion of $\approx 2.3 \text{\AA pixel}^{-1}$ and the spectral resolution full width at half-maximum (FWHM) of $\approx 7 \text{\AA}$. The slit was oriented at the parallactic angle because there was no possibility to select a position angle (PA) at this telescope. Three exposures of 900 s and 1200 s were taken during the first and second nights, respectively, with a seeing of ≈ 1.0 –1.3 arcsec. The data were reduced in a standard way using the MIDAS and IRAF software. All one-dimensional (1D) spectra obtained during the two nights were then averaged to produce a final spectrum (see the lower curve in

Fig. 2). The spectrum shows the $H\alpha$ and $H\beta$ emission lines and numerous singly ionized iron emission lines, typical of LBVs near the brightness maximum (e.g. Stahl et al. 2001). In the red part of the spectrum we detected the prominent O I $\lambda 7771$ –4 \AA triplet in absorption (not shown in Fig. 2), which is a good indicator of luminosity (Merrill 1934). The equivalent width (EW) of this triplet of $1.93 \pm 0.18 \text{\AA}$ implies that MN44 is a supergiant star of luminosity class Ia (e.g. Keenan & Hynek 1950; Osmer 1972). These findings along with the presence of the circular shell around the star allowed us to classify MN44 as a cLBV.

To search for possible spectral variability of MN44, we obtained four more spectra with the Southern African Large Telescope (SALT; Buckley, Swart & Meiring 2006; O’Donoghue et al. 2006) on 2015 May 6, June 14, August 2 and September 8 (see Table 1 for the log of our spectroscopic observations of MN44). The spectra were taken with the Robert Stobie Spectrograph (RSS; Burgh et al. 2003; Kobulnicky et al. 2003) in the long-slit mode with a 1.25'' slit width. The PG900 grating was used on May 6, August 2 and September 8 to cover the spectral range of 4200–7300 \AA . We used the same grating on June 14 to cover the spectral range of 4350–7450 \AA , which allowed us to fill gaps in the wavelength coverage of the three other spectra. The final reciprocal dispersion and FWHM spectral resolution of the spectra are $0.97 \text{\AA pixel}^{-1}$ and $4.51 \pm 0.13 \text{\AA}$, respectively. The RSS uses a mosaic of three 2048 \times 4096 CCDs and the final spatial scales for observations were $0.51'' \text{ pix}^{-1}$ in the first night and $0.25'' \text{ pix}^{-1}$ in the next three nights. The corresponding seeing was of ≈ 1.0 , 2.5, 2.0 and 1.4 arcsec. Two exposures were taken each night. The short exposures were used to avoid saturation of the extremely strong $H\alpha$ emission line. In all observations the slit was oriented at PA=43° (measured from north to west) in order to cross the region of bright emission (knot) to the northwest of MN44. A Xe lamp arc spectrum was taken immediately after the science frames. A spectrophotometric standard star was observed during twilight time for relative flux calibration. The primary reduction of the data was done with the SALT science pipeline (Crawford et al. 2010). After that, the bias and gain corrected and mosaiced long-slit data were reduced in the way described in Kniazev et al. (2008). The resulting normalized spectra are presented in Fig. 2 (see the upper four curves). In the figure we show only parts of the spectra longward of $\approx 4800 \text{\AA}$ because most of the SALT spectra were taken during bright time and their blue parts are very noisy and do not contain meaningful information.

To detect photometric variability of MN44, we determined its B , V and I_c magnitudes on CCD frames obtained with the SAAO 76-cm telescope in 2012–2014. We used an

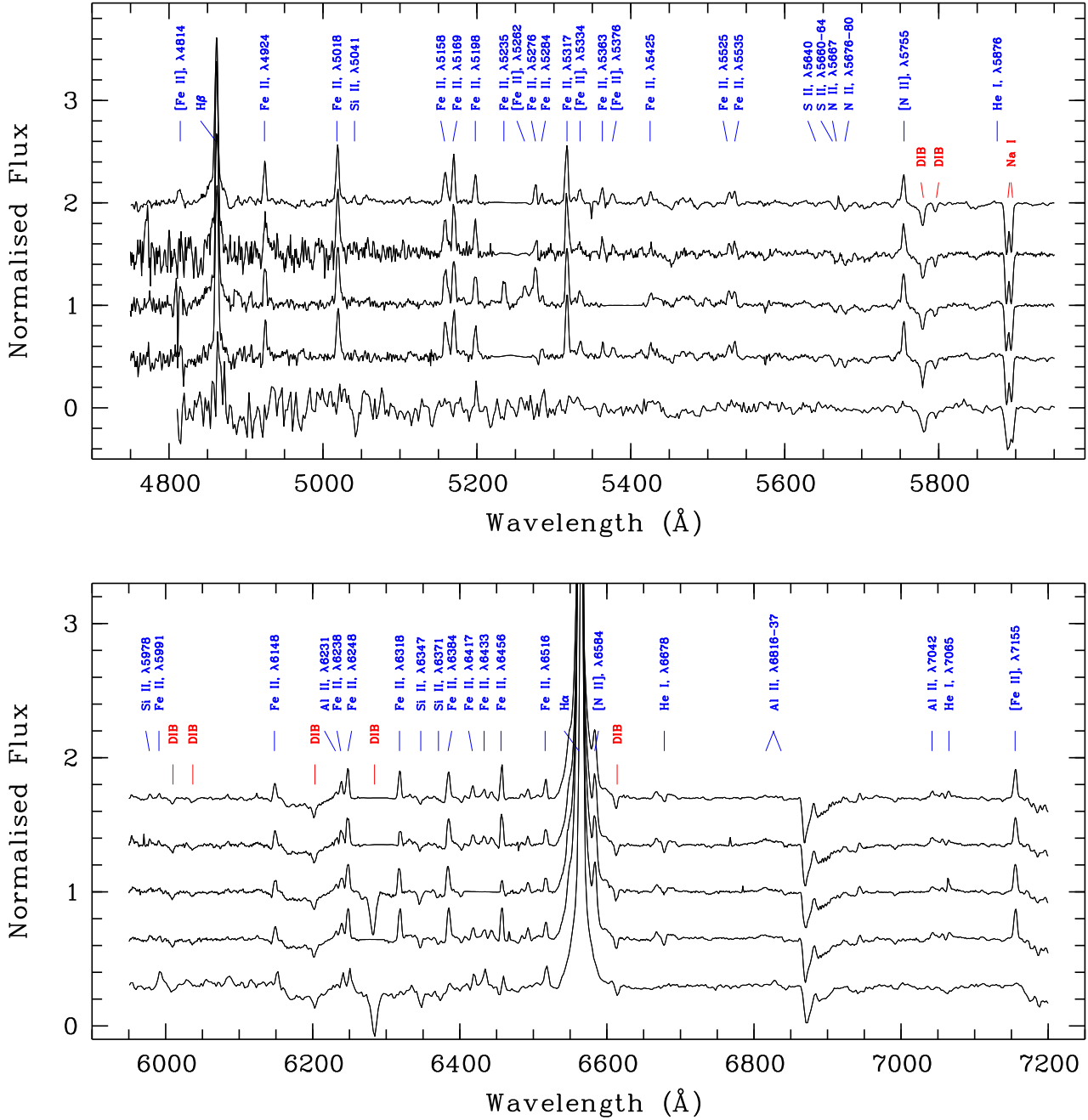


Figure 2. Normalized spectra of MN44 obtained in 2009 with the SAAO 1.9-m telescope (the lower curve) and on 2015 May 6, June 14, August 2 and September 8 with the SALT (four upper curves with the date increasing from bottom to top). The principal lines and most prominent DIBs are indicated.

SBIG ST-10XME CCD camera equipped with BVI_c filters of the Kron-Cousins system (see e.g. Berdnikov et al. 2012) to build the system of secondary standards in the field of MN44. With these standards, we derived V and I_c magnitudes of MN44 using images obtained with the SAAO 1-m telescope on 2015 May 19, and an I_c magnitude using acquisition images obtained with the SALT on 2015 June 14, August 2 and September 8. We also calibrated the 1.9-m telescope spectrum and synthesized its V magnitude in

the way described in Kniazev et al. (2005). Using the same standards, we recalibrated the I and B magnitudes from the USNOB-1 catalogue (Monet et al. 2003). The results are presented in Table 2. To this table we also added the lower limit on the V magnitude given in Vega et al. (1980), J and K_s magnitudes from 2MASS and two-epoch I , J and K_s photometry from the Deep Near Infrared Survey of the Southern Sky (DENIS; The DENIS Consortium, 2005).

Table 2. Photometry of MN44.

Date	B	V	I_c	$V - I_c$	J	K_s
1974 May ⁽¹⁾	–	> 15.58	–	–	–	–
1980 May 23 ⁽²⁾	–	–	13.3±0.2	–	–	–
1982 August 8 ⁽²⁾	18.9±0.3	–	–	–	–	–
1998 July 1 ⁽³⁾	–	–	11.84±0.03	–	9.01±0.07	7.42±0.06
1998 November 3 ⁽³⁾	–	–	11.74±0.03	–	8.90±0.08	7.28±0.06
1999 June 18 ⁽⁴⁾	–	–	–	–	8.41±0.02	6.81±0.03
2009 May 31 ⁽⁵⁾	–	14.41±0.04	10.20±0.10	4.21±0.11	–	–
2012 May 5 ⁽⁶⁾	–	14.75±0.01	10.46±0.01	4.29±0.01	–	–
2013 January 13 ⁽⁶⁾	17.86±0.20	14.99±0.01	10.74±0.01	4.25±0.01	–	–
2014 April 25 ⁽⁶⁾	18.58±0.08	15.67±0.03	11.47±0.01	4.20±0.03	–	–
2015 May 19 ⁽⁷⁾	–	15.70±0.03	11.77±0.05	3.93±0.06	–	–
2015 June 14 ⁽⁸⁾	–	–	11.81±0.06	–	–	–
2015 August 2 ⁽⁸⁾	–	–	11.70±0.05	–	–	–
2015 September 8 ⁽⁸⁾	–	–	11.65±0.04	–	–	–

(1) Vega et al. (1980); (2) USNO B-1; (3) DENIS; (4) 2MASS; (5) 1.9-m telescope; (6) 76-cm telescope; (7) 1-m telescope; (8) SALT.

4 DISCUSSION

4.1 MN44: a bona fide LBV

Fig. 2 shows a montage of five spectra obtained in 2009 and 2015 with the principal lines and most prominent diffuse interstellar bands (DIBs) indicated. All wavelengths are given in air. The lower curve represents the averaged spectrum based on two observations carried out on 2009 May 31 and June 2 with the SAAO 1.9-m telescope. Four other curves (from bottom to top) correspond to spectra taken with the SALT on 2015 May 6, June 14, August 2 and September 8. EWs, FWHMs and heliocentric radial velocities (RVs) of some lines in the spectra (measured applying the MIDAS programs; see Kniazev et al. 2004 for details) are given in Table 3.

Comparison of the spectra shows that in 2015 the EWs of the $H\alpha$ and $H\beta$ lines increased by ≈ 3 and 6–9 times, respectively, compared to 2009 (see also Table 3), while the broad Thomson scattering wings of these lines became even more broader. Some Fe II lines already present in the 2009’s spectrum, e.g. at $\lambda\lambda 5317, 6384, 6456$, became very prominent in 2015. The forbidden lines of [N II] $\lambda 5755$ and [Fe II] $\lambda\lambda 5334, 5376$ and 7155 increased their strength as well, and the [N II] $\lambda 6584$ line became very prominent on the red wing of the $H\alpha$ line. More importantly, the 2015’s spectra show emergence of the He I lines $\lambda\lambda 5876, 6676$ and 7065 . These lines were absent in the first epoch spectrum, but show up in 2015 May 6 as central absorptions accompanied by blue and red emission wings. The presence of these lines imply that the star became hotter during the last six years, which is expected in view of the significant decline of the stellar brightness during the same time period (see below). Fig. 3 plots the evolution of the He I $\lambda 6676$ line profile with time. One can see that the central absorption became less deep in June 14, then returned to almost the same state as it was in May 6 and then again became less deep, while the emission wings remain almost intact.

The [Fe II] $\lambda 5376$ line in the spectra taken on 2015 May 6 and September 8 has a distinct flat-topped profile. This indicates that the line is formed in a region of constant expansion velocity and therefore its FWHM (respectively, 5.39 ± 0.26

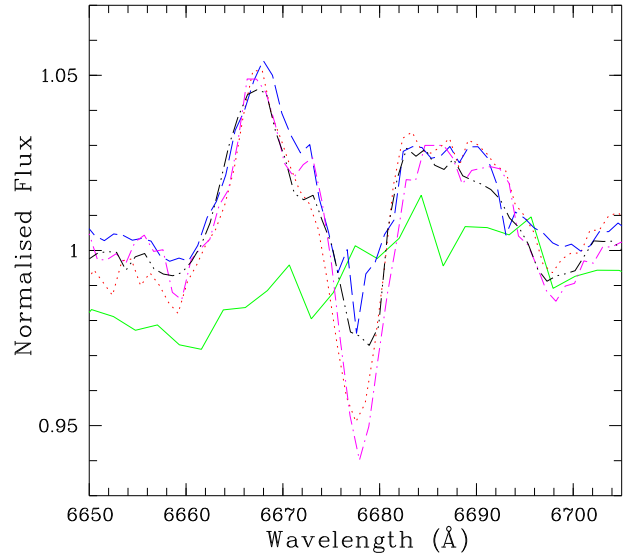


Figure 3. Evolution of the He I $\lambda 6678$ line profile with time: 2009 May 31 – June 2 (solid green line), 2015 May 6 (dotted red line), 2015 June 14 (dashed blue line), 2015 August 2 (dash-dotted violet line) and 2015 September 8 (dash-dot-dotted black line).

\AA and $5.48\pm 0.32 \text{ \AA}$) could be used to estimate the terminal wind velocity, v_∞ (Stahl et al. 1991). After correction for instrumental width, one finds $v_\infty = 165\pm 29$ and $174\pm 33 \text{ km s}^{-1}$. The wind velocity could also be estimated by using the FWHM of the [N II] $\lambda 5755$ line (e.g. Crowther, Hillier & Smith 1995). After correction for instrumental width, the FWHMs of $4.81\pm 0.27 \text{ \AA}$ (2015 June 14), $5.04\pm 0.26 \text{ \AA}$ (2015 August 2) and 5.05 ± 0.20 (September 8) correspond to v_∞ of $87\pm 45, 117\pm 33$ and $118\pm 21 \text{ km s}^{-1}$, respectively. Note that although all five estimates agree with each other within the error margins, the lower values of v_∞ based on the [N II] line might be because this line originates closer to the star where the wind is still accelerated (Stahl et al. 1991). This supposition is supported by the observed [N II] $\lambda\lambda 5755, 6584$ line

Table 3. EWs, FWHMs and RVs of some lines in the spectra of MN44.

λ_0 (Å) Ion	EW(λ) (Å)	FWHM(λ) (Å)	RV (km s ⁻¹)
2009 May 31 – June 2 (averaged)			
4861 H β	1.46 \pm 0.50	5.41 \pm 2.12	206 \pm 58
6347 Si II	-0.25 \pm 0.15	—	35 \pm 15
6371 Si II	-0.19 \pm 0.15	—	—
6563 H α	38.41 \pm 1.70	8.05 \pm 0.41	134 \pm 16
2015 May 6			
4861 H β	9.24 \pm 0.26	5.18 \pm 0.16	60 \pm 15
5334 [Fe II]	0.61 \pm 0.03	5.74 \pm 0.31	53 \pm 15
5376 [Fe II]	0.53 \pm 0.03	5.39 \pm 0.26	50 \pm 15
5755 [N II]	1.68 \pm 0.09	4.48 \pm 0.27	9 \pm 14
6347 Si II	-0.29 \pm 0.03	4.17 \pm 0.29	-26 \pm 11
6371 Si II	-0.08 \pm 0.02	4.78 \pm 0.40	-8 \pm 11
6563 H α	112.01 \pm 1.62	5.15 \pm 0.09	57 \pm 11
7155 [Fe II]	1.15 \pm 0.03	5.04 \pm 0.09	32 \pm 10
2015 June 14			
4861 H β	12.62 \pm 0.50	5.53 \pm 0.25	53 \pm 16
5334 [Fe II]	0.54 \pm 0.08	6.21 \pm 0.62	16 \pm 20
5755 [N II]	1.59 \pm 0.11	4.81 \pm 0.27	-21 \pm 14
6347 Si II	-0.49 \pm 0.08	5.62 \pm 0.22	-83 \pm 12
6371 Si II	-0.08 \pm 0.06	4.76 \pm 0.60	-68 \pm 12
6563 H α	117.92 \pm 1.92	5.31 \pm 0.10	43 \pm 11
7155 [Fe II]	1.18 \pm 0.08	5.19 \pm 0.10	6 \pm 10
2015 August 2			
4861 H β	9.81 \pm 0.50	5.14 \pm 0.30	23 \pm 11
5334 [Fe II]	0.23 \pm 0.09	6.51 \pm 1.18	-67 \pm 26
5376 [Fe II]	0.32 \pm 0.09	3.80 \pm 0.61	17 \pm 16
5755 [N II]	1.46 \pm 0.13	5.04 \pm 0.26	-31 \pm 8
6347 Si II	-0.03 \pm 0.07	3.17 \pm 0.23	-87 \pm 7
6371 Si II	-0.02 \pm 0.07	3.07 \pm 0.63	-65 \pm 7
6563 H α	104.11 \pm 1.84	5.27 \pm 0.11	27 \pm 6
7155 [Fe II]	1.08 \pm 0.11	5.38 \pm 0.11	-2 \pm 5
2015 September 8			
4815 [Fe II]	0.78 \pm 0.07	5.98 \pm 0.59	-38 \pm 20
4861 H β	12.16 \pm 0.47	5.60 \pm 0.25	-14 \pm 14
5334 [Fe II]	0.49 \pm 0.02	5.28 \pm 0.22	-24 \pm 12
5376 [Fe II]	0.45 \pm 0.03	5.48 \pm 0.32	-37 \pm 13
5755 [N II]	1.24 \pm 0.05	5.05 \pm 0.20	-45 \pm 11
6347 Si II	-0.10 \pm 0.05	4.60 \pm 0.34	-66 \pm 9
6563 H α	102.16 \pm 1.92	4.71 \pm 0.10	-4 \pm 11
7155 [Fe II]	1.16 \pm 0.02	4.92 \pm 0.09	-16 \pm 9

Note: The negative EWs correspond to absorption lines.

intensity ratio, which implies that the nitrogen forbidden lines originate in a dense ($\geq 10^7$ cm⁻³) matter (e.g. Tarter 1969), probably close to the star (cf. Stahl et al. 1991). Note also that the low wind velocity of MN44 during its minimum light phase suggests that this star is close to the Eddington limit, probably because it already lost a significant fraction of its initial mass either in a single giant eruption or in a number of less catastrophic mass-loss episodes (Humphreys et al. 2014a,b).

The forbidden lines can also be used to derive the systemic velocity (Stahl et al. 2001). Inspection of Table 3, however, shows significant changes in RVs of the [Fe II] and [N II] lines from spectrum to spectrum. One can see that the RVs

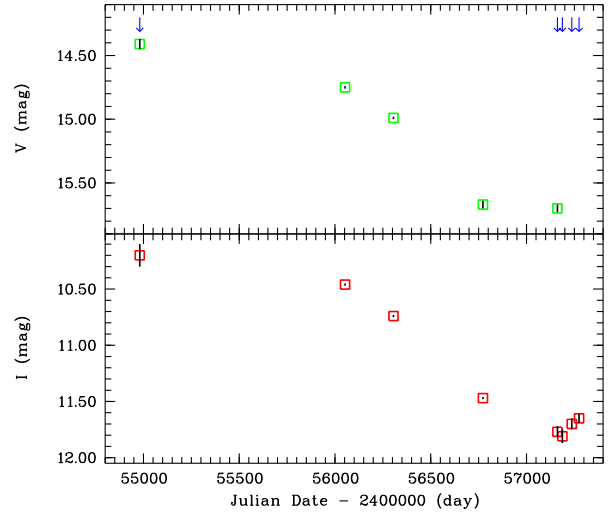


Figure 4. Light curves of MN44 in the V and I bands. 1σ error bars are indicated, but in most cases they are within the size of the data points (boxes). The arrows mark the dates of the spectroscopic observations.

of most of these lines systematically reduced during the last four months and that the velocity decrease was more prominent during the first month. RVs of the Si II $\lambda\lambda$ 6347, 6371 absorption doublet and the Balmer lines also demonstrate the same trend. The decrease in the RVs of the Balmer lines would be much more stronger if one takes into account the 2009's spectrum. Although these changes suggest that MN44 might be a close eccentric binary system (cf. Section 4.4), the limited available data did not allow us to prove this for sure.

The detected spectral variability of MN44 strongly suggests that this star is a bona fide LBV, currently evolving towards the hot state, i.e. towards the brightness minimum (e.g. Stahl et al. 2001). This implication is reinforced by photometric measurements given in Table 2, which show that MN44 has experienced strong brightness decline during the period of our spectroscopic observations. This is illustrated by Fig. 4, which plots V - and I_c -band light curves of MN44 since its identification as a cLBV in 2009 with arrows indicating times when the spectra were obtained. For each data point (square) we give 1σ error bars, which in most cases are less than the size of the squares themselves. Fig. 4 shows that MN44 became fainter in the V and I_c bands, respectively, by ≈ 1.3 and 1.6 mag during the last 6 years. One can see also that the I_c -band brightness of MN44 has reached minimum in 2015 June and then starts to increase. On a longer time-scale, the I_c -band variability is even more striking. From Table 2 it follows that MN44 has brightened by ≈ 3 mag (!) during ≈ 30 yr preceding our monitoring campaign. The large magnitude of the I_c -band excursion suggests that MN44 might belong to a rare group of LBVs exhibiting giant eruptions (as in η Car and P Cyg) during which their bolometric luminosity changes (Humphreys & Davidson 1994). Table 2 also shows that MN44 became brighter in the J and K_s bands by ≈ 0.6 mag during ≈ 7.5 months in 1998–1999.

By using the weighted least square approximation, we found that the $V-I_c$ colour of MN44 has decreased by ≈ 0.3 mag during the last six years. On the other hand, as one can

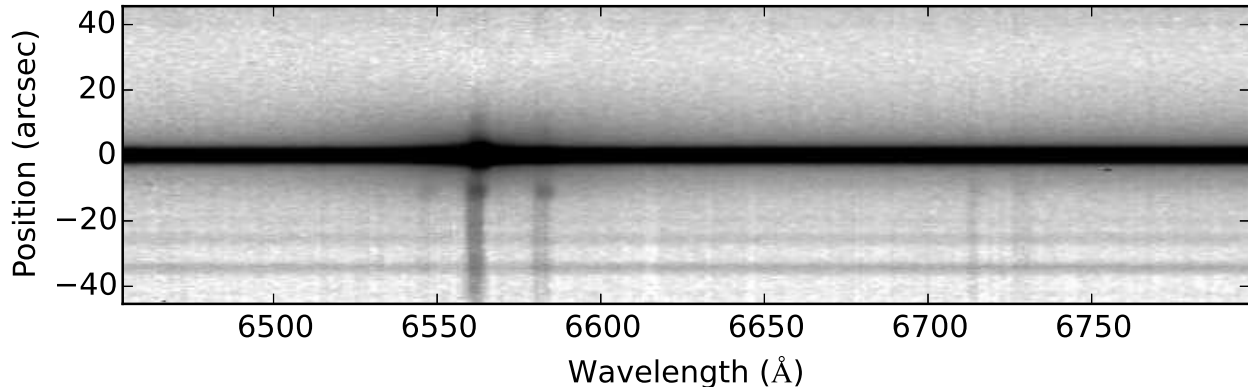


Figure 5. A part of the 2D spectrum of the diffuse emission around MN44 (obtained on 2015 June 14), showing nebular emission lines (from left to right) of [N II] $\lambda 6548$, H α , [N II] $\lambda 6584$ and [S II] $\lambda\lambda 6717, 6731$. The lower part of the spectrum corresponds to the emission northwest of MN44. The lines in this direction have two distinct velocity components, namely, in the inner region ($\lesssim 14$ arcsec from MN44) they are shifted to the red end of the spectrum compared to the lines originated at larger angular distances (outer region). The upper part of the spectrum corresponds to the emission southeast of MN44, which extends from the star for ≈ 10 arcsec. See Fig. 6 and text for details.

infer from Table 2, this decrease has occurred mostly during the last year, while in 2009–2014 the colour did not change much despite of significant (>1 mag) brightness decrease of the star. Such behaviour is not typical of LBV excursions at constant bolometric luminosity during which stars become bluer with the brightness decrease, but it was observed for LBVs showing changes in the bolometric luminosity (e.g. Clark et al. 2009; Kniazev et al. 2015). Whether this is the case for MN44 as well could be proved with a detailed spectral modelling, which is, however, beyond the scope of this paper.

Taken together, our observations of MN44 unambiguously show that this star is a new (seventeenth) member of the family of Galactic bona fide LBVs (see Kniazev et al. 2015 for a recent census of these objects).

4.2 H α + [N II] emission to the northwest of MN44

The SHS H α + [N II] image presented in Fig. 1 shows that there is a diffuse emission immediately around MN44 and further northwest from it. There is also a bright knot of emission apparently in contact with the circumstellar shell. To clarify the nature of the emission around MN44, we obtained long-slit SALT spectra with the slit oriented at PA= 43° in order to cross the knot. In two-dimensional (2D) spectra the knot appears as emission lines of H β , H α , [N II] $\lambda\lambda 6548, 6584$ and [S II] $\lambda\lambda 6717, 6731$. In the following, we use the spectrum taken on 2015 May 6 because of its better quality. A part of this spectrum is presented in Fig. 5. One can see two distinct velocity components in the emission lines. The lines produced in the inner region (≤ 14 arcsec from MN44, i.e. within the confines of the $24 \mu\text{m}$ shell) are shifted to the red end of the spectrum compared to the lines originated at larger angular distances from the star (outer region).

1D spectra of the inner and outer regions were extracted by summing up, without any weighting, all rows in angular distance intervals from ≈ 9 to 14 arcsec and from 14 to 40 arcsec, respectively (see Fig. 6). The emission lines detected

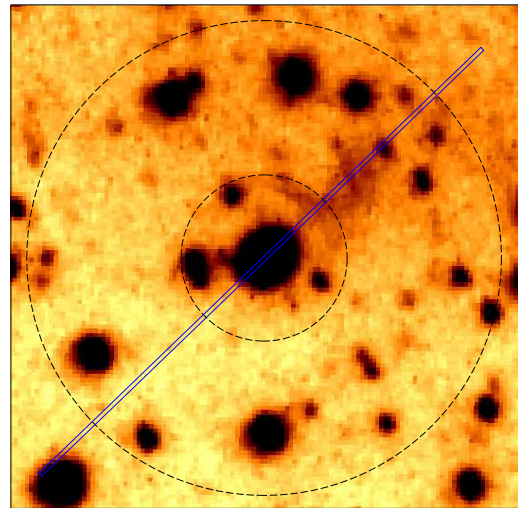


Figure 6. SHS image of MN44 and the diffuse H α + [N II] emission around it with the orientation of the RSS slit (PA= 43°) shown by a (blue) rectangle. Concentric, dashed circles of radius of 14 and 40 arcsec are overlotted on the image to show the extraction regions of the 1D spectra of the diffuse emission to the northwest of MN44. Note that the radius of the inner circle is almost equal to the radius of the $24 \mu\text{m}$ circumstellar shell. See text for details.

in these spectra were measured using the programs described in Kniazev et al. (2004). Table 4 lists the observed intensities of the lines normalized to H β , $F(\lambda)/F(\text{H}\beta)$, the reddening-corrected line intensity ratios, $I(\lambda)/I(\text{H}\beta)$, the logarithmic extinction coefficients, $C(\text{H}\beta)$, the colour excesses, $E(B - V)$, and the heliocentric radial velocities, v_{hel} , of the two regions. The 1D spectrum of the inner region is shown in Fig. 7.

The [S II] $\lambda\lambda 6716, 6731$ line intensity ratio can be used to derive the electron number density, n_e , in the line-emitting gas (Krueger, Aller & Czyzak 1970; Saraph &

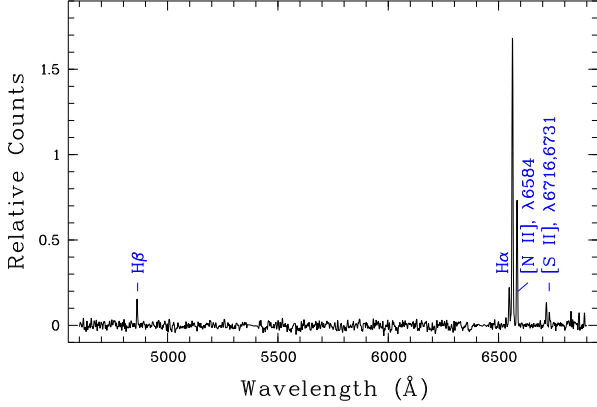


Figure 7. 1D spectrum of the knot to the northwest of MN44 obtained on 2015 June 14.

Table 4. Line intensities in the spectra of diffuse emission to the northwest of MN44.

λ_0 (Å)	Ion	$F(\lambda)/F(H\beta)$	$I(\lambda)/I(H\beta)$
inner region			
4861	H β	1.00 \pm 0.10	1.00 \pm 0.10
6548	[N II]	1.97 \pm 0.15	0.40 \pm 0.03
6563	H α	14.56 \pm 1.04	2.92 \pm 0.23
6584	[N II]	5.69 \pm 0.41	1.12 \pm 0.09
6717	[S II]	0.97 \pm 0.11	0.17 \pm 0.02
6731	[S II]	0.49 \pm 0.08	0.09 \pm 0.02
C(H β) dex			
		2.10 \pm 0.09	
$E(B - V)$			
		1.43 \pm 0.06 mag	
v_{hel}			
		-11 \pm 6 km s $^{-1}$	
outer region			
4861	H β	1.000 \pm 0.291	1.000 \pm 0.299
6548	[N II]	0.745 \pm 0.234	0.196 \pm 0.066
6563	H α	11.170 \pm 2.316	2.908 \pm 0.673
6584	[N II]	2.269 \pm 0.504	0.583 \pm 0.144
6717	[S II]	1.270 \pm 0.355	0.300 \pm 0.091
6731	[S II]	1.028 \pm 0.316	0.241 \pm 0.080
C(H β)			
		1.76 \pm 0.27	
$E(B - V)$			
		1.20 \pm 0.18 mag	
v_{hel}			
		-39 \pm 12 km s $^{-1}$	

Seaton 1970). In the inner region, the measured ratio of $1.89^{+0.82}_{-0.53}$ agrees at 1 sigma level with the theoretical upper limit on this ratio of ≈ 1.4 (Krueger et al. 1970). Thus, one can only put an upper limit on n_e of $\leq 10 \text{ cm}^{-3}$. In the outer region, the line ratio of $1.24^{+1.19}_{-0.59}$ corresponds to $n_e = 190^{+2770}_{-180}$.

The above estimates of $C(H\beta)$ and $n_e([S II])$ were derived for the Case B recombination and under the assumption that the electron temperature, T_e , is equal to 10^4 K.

The [N II] and [S II] line intensities can be used to estimate the nitrogen to sulphur abundance ratio, $N(N^+)/N(S^+)$, which is almost independent of n_e and T_e , provided that $n_e \leq 1000 \text{ cm}^{-3}$ and $T_e \leq 10^4$ K. In this case,

it is given by (see Benvenuti, D’Odorico & Peimbert 1973 and references therein):

$$\frac{N(N^+)}{N(S^+)} = 3.61 \frac{I(6584)}{I(6716 + 6731)}. \quad (1)$$

Using equation (1) and Table 4, one finds $N(N^+)/N(S^+) \approx 15.55^{+4.31}_{-3.16}$ and $3.89^{+3.20}_{-1.66}$ for the inner and outer regions, respectively. The former ratio is $\approx 3.0^{+0.9}_{-0.6}$ times larger than the solar value of 5.12 (Asplund et al. 2009), while the latter one is comparable to it. The high $N(N^+)/N(S^+)$ ratio in the inner region could be owing to pollution by CNO-processed ejecta from MN44. Since the sulfur abundance is not expected to change during stellar evolution, one can argue that the inner region is enriched in N by a factor of $\approx 2-4$. This provides further support to the physical association between the knot and the circumstellar shell around MN44. The solar abundance of N in the outer region suggests that it is an H II region.

Since the $E(B - V)$ values for the inner and outer regions are consistent with each other within the error margins, it is likely that both are located at the same distance and ionized by MN44 during its hot state. If so, then the difference in the heliocentric radial velocities of the two regions could be understood if the inner part of the knot was accelerated because of interaction with the circumstellar shell of MN44. This, in turn, would imply that the radial velocity of the shell (and MN44) relative to the H II region is $28 \pm 13 \text{ km s}^{-1}$.

4.3 Reddening to and luminosity of MN44

The colour excess towards the knot could be used to derive the V -band extinction, A_V , in the direction of MN44, and thereby to constrain the absolute visual magnitude, M_V , of this star. For the standard ratio of total to selective extinction of $R_V = 3.1$, one finds $A_V = 4.43$ mag, while for M_V one has the following equation:

$$M_V = V - DM - A_V, \quad (2)$$

where DM is the distance modulus. Using equation (2) and the V -band magnitude of MN44 of 15.69 (measured on 2015 May 19), one has $M_V = 11.26 - DM$ mag. To further constrain M_V , we note that the sightline towards MN44 first enters the Carina-Sagittarius arm (located at a distance of ~ 2.1 kpc from the Sun), then (at ~ 3.3 kpc) intersects the Crux-Scutum arm, then twice crosses the Norma arm (at ~ 5.5 and 10.8 kpc), and then again crosses the Crux-Scutum and Carina-Sagittarius arms (at ~ 15 and 19 kpc, respectively) (e.g. Cordes & Lazio 2002). The distances at which the sightline intersects the spiral arms correspond to DM values of $\approx 11.61, 12.59, 13.70, 15.17, 15.88$ and 16.39 mag, respectively. One can see that M_V of MN44 would be at the upper end of values typical of B supergiants even if this star is located in the more distant part of the Carina-Sagittarius arm (DM=16.39 mag), i.e. $M_V \approx -5.1$ mag. To derive the bolometric luminosity of MN44, we note that the 2015’s spectra of this star are very similar to those of the LBV WS1 in the cool state, for which we derived the effective temperature, T_{eff} , of ≈ 12000 K (Kniazev et al. 2015). At this temperature, the bolometric correction of MN44 is equal to ≈ -0.8 mag. Correspondingly, the bolometric luminosity of MN44 (for DM=16.39 mag) would be only of $\log(L_{\text{bol}}/L_{\odot}) \approx 4.3$,

which is much smaller than the minimum value of 5.1 ever derived for known bona fide or cLBVs (Humphreys et al. 2014a).

The reddening towards MN44 could also be estimated by matching the dereddened spectral slope of this star with those of stars of similar T_{eff} . Using the Stellar Spectral Flux Library by Pickles (1998), we found $E(B - V) = 3.30 \pm 0.10$ mag (this estimate only slightly depends on the assumed T_{eff} ; see Gvaramadze et al. 2012a) and $A_V = 10.23$ mag. Correspondingly, one has $M_V = 5.46 - DM$ mag. One can see that MN44 would have a reasonable luminosity, i.e. $\log(L_{\text{bol}}/L_{\odot}) \geq 5.1$, if the star is located at $d \geq 3.3$ kpc, i.e. in the near segment of the Crux-Scutum arm or further out ($DM \geq 12.59$ mag; see Table 5). At these distances, MN44 would be located on the cool side of the S Dor instability strip (Wolf 1989; Groh et al. 2009) on the Hertzsprung-Russell diagram.

The A_V value derived from the spectral slope of MN44 exceeds by ≈ 5.8 mag the extinction derived towards the knot. A trivial explanation of this discrepancy is that MN44 and the knot are located at different distances and are simply projected by chance along the same line-of-sight. This explanation, however, is unlikely because there are strong indications that the knot is in a contact with the circumstellar shell of MN44. Instead, one can envisage two other possible explanations.

Our preferred explanation of the large discrepancy in the A_V values is that MN44 is shrouded by dense circumstellar material and that this material significantly contributes to the extinction of the star. For example, the dusty material of the Homunculus nebula is responsible for ≈ 4 mag of the V-band extinction towards η Car (Humphreys, Davidson & Smith 1999; cf. van Genderen, de Groot & The 1994). It is, therefore, possible that the dusty ejecta from recent outbursts of MN44 causes the excess extinction towards this star as well. If this explanation is correct, then one can expect that the changes in the brightness of MN44 might be caused not only by the intrinsic variability of the star itself, but also by the changeable circumstellar extinction (cf. van Genderen et al. 1994). Or else the extra extinction might be due to a dense circumbinary disk if MN44 is a binary system (see Section 4.4).

An alternative explanation of the discrepancy is that the intrinsic Balmer decrement in the spectrum of the knot is much shallower than what follows from the standard Case B recombination model, i.e. the intrinsic value of the $I(\text{H}\alpha)/I(\text{H}\beta)$ ratio is significantly smaller than ≈ 3 . For this explanation to work, the H emission should arise in a very dense medium with $n_e \gtrsim 10^{13} \text{ cm}^{-3}$ (Drake & Ulrich 1980). This requirement does not contradict to the low electron density indicated by the $[\text{S II}] \lambda\lambda 6716, 6731$ line intensity ratio because these forbidden lines could originate in a low-density halo around the dense core of the knot. If the H emission indeed originates in the very dense medium, then the $I(\text{H}\alpha)/I(\text{H}\beta)$ ratio could be as small as ≈ 1 (see fig. 7 in Drake & Ulrich 1980), which for the line intensities observed in the spectrum of the knot would result in a factor of ≈ 2 larger values of $E(B - V)$ and A_V , thereby bringing them closer to the values derived from the dereddening the spectral slope of MN44. To check this explanation, one has to measure more Balmer line ratios in the spectrum of the knot, which requires much more deep spectroscopic observations.

An additional constraint on the distance to MN44 comes from the empirical amplitude-luminosity relation of LBVs, which implies that the amplitude of photometric variability increases with L_{bol} (Wolf 1989). The strong changes in the brightness of MN44 suggest that the luminosity of this star should be well above the lower end of the range of luminosities derived for (c)LBVs. This means that the star should be located at least in the Norma arm or in the next arms out, i.e. at $d \geq 5.5$ kpc. At these distances, MN44 would lie at ≥ 110 pc below the Galactic plane. This separation from the plane is comparable to or larger than the exponential scale height of runaway O stars of ≈ 90 pc (Stone 1979) and is at least a factor of two larger than that of “normal” OB stars (Stone 1979; Reed 2000). Thus, MN44 might be a runaway star; we further discuss this possibility in Section 4.5.

On the other hand, the larger the distance to MN44, the larger its luminosity and initial mass, M_{init} , the shorter the lifetime of this star, t , and the larger its separation from the Galactic plane, $h = d \sin b$ (see Table 5). This means that the more massive the star the higher the peculiar velocity perpendicular to the Galactic plane, $\sim h/t$, it should have (see Table 5). For example, if MN44 is located at $d = 15$ kpc ($M_{\text{init}} \approx 120 M_{\odot}$) then its short lifetime of $t \sim 3$ Myr would imply that to reach the height of $h \approx 300$ pc, the star should be ejected from the parent cluster with a velocity of $\approx 100 \text{ km s}^{-1}$ (provided that the ejection event has occurred soon after the star was born). Although ejection of such massive and high-velocity stars is not impossible, the probability of these events is very low (Gvaramadze & Guandris 2011). It would be even much lower if MN44 is a massive binary system (see next section).

Finally, the distance to MN44 could also be constrained through the kinematic distance to the H II region northwest of the star (in Sect. 4.2, we argue that they are likely located at the same distance). Using the heliocentric radial velocity of the H II region of $-39 \pm 12 \text{ km s}^{-1}$, adopting the radial velocity dispersion of H II regions within an arm of $\sim 10 \text{ km s}^{-1}$ (Georgelin & Georgelin 1976), and assuming the distance to the Galactic Centre of $R_0 = 8.0$ kpc and the circular rotation speed of the Galaxy of $\Theta_0 = 240 \text{ km s}^{-1}$ (Reid et al. 2009), and the solar peculiar motion $(U_{\odot}, V_{\odot}, W_{\odot}) = (11.1, 12.2, 7.3) \text{ km s}^{-1}$ (Schönrich, Binney & Dehnen 2010), one finds a kinematic distance of $\approx 2.3_{-1.4}^{+1.1}$ or $12.1_{-1.1}^{+1.4}$ kpc. For the distance range implied by the error margins of the former distance estimate, the luminosity of MN44 would be unrealistically low (see above). The error margins of the latter distance estimate allow the possibility that MN44 is located in the outer segment of the Norma arm. In this case, the bolometric luminosity of MN44 of $\log(L_{\text{bol}}/L_{\odot}) = 6.1$ would exceed the Humphreys-Davidson luminosity limit (Humphreys & Davidson 1979), i.e. the star would be located in a region of the Hertzsprung-Russell diagram where the massive stars are expected to experience unsteady (eruptive) high mass-loss episodes. We caution however, that the possible association between the optically visible knot and the circumstellar shell is rather indicative of moderate (≈ 4 mag) interstellar extinction towards MN44, which in turn suggests that this star is located at a shorter distance, i.e. in the inner segment of the Norma arm. In fact, the above kinematic distance estimates would be meaningless if the H II region has a peculiar radial velocity of several

Table 5. MN44: absolute visual magnitude, luminosity, initial mass, lifetime, height below the Galactic plane, and peculiar velocity perpendicular to the Galactic plane for different distances/distance moduli and $A_V = 10.23$ mag. See text for details.

d (kpc)	DM (mag)	M_V (mag)	$\log(L_{\text{bol}}/L_{\odot})$	M_{init} (M_{\odot})	t (Myr)	h (pc)	h/t (km s^{-1})
2.1	11.61	-6.2	4.7	15	12	40	3
3.3	12.59	-7.1	5.1	20	9	70	8
5.5	13.70	-8.2	5.5	35	6	110	18
10.8	15.17	-9.7	6.1	60	4	220	55
15	15.88	-10.4	6.4	120	3	300	100
19	16.39	-10.9	6.6	150	2.5	380	150

tens of km s^{-1} , e.g. because of interaction with the stellar wind/ejecta during the previous mass-loss episodes.

4.4 MN44: a massive X-ray binary?

In Section 2, we noted that Masetti et al. (2010) identified MN44 as a counterpart of the *INTEGRAL* source of hard X-ray emission IGR J16327–4940 and tentatively classified this source as a HMXB. Let us discuss whether the LBV classification of MN44 is consistent with the possibility that this object is a source of hard X-ray emission.

First, we list some relevant data on IGR J16327–4940 given in the Fourth soft gamma-ray source catalogue obtained with the IBIS gamma-ray imager on board the *INTEGRAL* satellite (Bird et al. 2010). In this catalogue, IGR J16327–4940 is indicated as a transient (strongly variable) source with the 20–40 and 40–100 keV band fluxes time-averaged over the total exposure time of 3319.3 ks (or ≈ 38.4 d) of $F(20-40) < 0.2$ mCrab and $F(40-100) = 0.4 \pm 0.1$ mCrab, respectively. The catalogue also gives the peak 20–40 keV band flux of $F_{\text{peak}}(20-40) = 2.1 \pm 0.7$ mCrab, i.e. the mean flux measured during the largest observed outburst, in which the source was detected at a maximum level of significance of $5.6\text{-}\sigma$.

The above fluxes translate to the X-ray-to-bolometric luminosity ratios of $\log[L_X(20-40)/L_{\text{bol}}] < -5.30$, $\log[L_X(40-100)/L_{\text{bol}}] = -4.91$ and $\log[L_X(20-40)/L_{\text{bol}}] = -4.28$, which are independent of the actual distance to MN44. These ratios should be compared with $\log[L_X/L_{\text{bol}}]$ values observed for other (c)LBVs.

Nazé, Rauw & Hutsemékers (2012) conducted a search for X-ray emission from the Galactic bona fide and cLBVs using available at that time data from the *XMM-Newton* and *Chandra* X-ray observatories, which covered 31 of 67 known objects of this type. Besides two already known X-ray sources η Car and NAME VI CYG 12, they reported detection of X-ray emission from two additional (c)LBVs, Cl* Westerlund 1 W 243 and GAL 026.47+00.02, as well as possible detections of two more (c)LBVs near the Galactic Centre, GCIRS 34W and GCIRS 33SE. For four (c)LBVs with confidently detected X-ray emission the following $\log[L_X/L_{\text{bol}}]$ values were derived: ~ -5 (η Car), -6.1 (NAME VI CYG 12), -5.95 (GAL 026.47+00.02) and $-7.0\dots 7.3$ (Cl* Westerlund 1 W 243). These values imply that the L_X/L_{bol} ratios of the first three stars are one or two orders of magnitude larger than those typical of single O stars (i.e. $\approx 10^{-7}$; e.g. Pallavicini et al. 1981; Sana et

al. 2006), whose X-ray emission is believed to originate because of shocks inside stellar winds (e.g. Owocki, Castor & Rybicki 1988; Feldmeier, Puls & Pauldrach 1997). Since the wind velocities of the majority of (c)LBVs ($\sim 100 \text{ km s}^{-1}$) are about an order of magnitude lower than those of O stars, the bright X-ray emission of the three stars cannot be caused by intrinsic wind shocks, but rather should originate in colliding winds (Usov 1992; Stevens, Blondin & Pollock 1992), i.e. these stars should be members of close massive binaries (Nazé et al. 2012). This assertion conforms with the observed hardness and variability of the X-ray emission from two of these stars – η Car and NAME VI CYG 12. Cl* Westerlund 1 W 243 is also likely to be a massive binary system because its slow wind cannot produce wind shocks strong enough to account for the observed X-ray emission. If so, then the X-ray emission from this object should originate in a companion O star (Nazé et al. 2012).

For the remaining 23 (c)LBVs observed with *Chandra* and *XMM-Newton*, only upper limits on their X-ray fluxes were obtained. In most cases, these limits imply that $\log[L_X/L_{\text{bol}}] < -5\dots 6$, which leaves the possibility that the corresponding stars might be X-ray bright close massive binaries. For five (c)LBVs very strong constraints on the X-ray emission were derived, $\log[L_X/L_{\text{bol}}] < -8.2\dots 9.4$, indicating that some (c)LBVs are intrinsically weak X-ray sources. Possible reasons for this are that these (c)LBVs are single stars and/or their X-ray emission is significantly attenuated by dense circumstellar material (Nazé et al. 2012).

The high values of $\log[L_X/L_{\text{bol}}]$ of MN44 along with the hardness and variability of its X-ray emission point to the possibility that this star is a colliding-wind binary. In this case, the observed X-ray emission should originate at the shock interface between colliding winds, while its variability could be due to changes in the strength of the shocks caused by the eccentricity of the binary orbit and/or the S Dor-like variability of wind parameters (velocity, mass-loss rate) of the LBV star. Interestingly, at the distance of 5.5 kpc, the 20–100 keV band X-ray luminosity of MN44 of $1.4 \times 10^{34} \text{ erg s}^{-1}$ would be comparable to that of η Car of $0.7 \times 10^{34} \text{ erg s}^{-1}$ (Leyder, Walter & Rauw 2008). In this energy range, the X-ray emission originates mostly from non-thermal processes. In the case of η Car, it is believed that its 20–100 keV band X-ray emission is dominated by inverse Compton scattering of stellar UV photons by electrons accelerated in the wind collision zone (Leyder et al. 2008). The same mechanism could be at work in MN44 as well.

If subsequent (optical or infrared) spectroscopic mon-

itoring will prove that MN44 forms a binary system with another massive star, then dedicated X-ray observations of this system would be desirable to search for orbital modulation of its X-ray emission (e.g. Nazé et al. 2007; Hamaguchi et al. 2014). The X-ray light curve, however, could not necessarily be periodic because the orbital modulation of the X-ray emission might be affected by changes in the wind of the LBV component of the binary (unless the SDor-like activity of MN44 is triggered by the effect of the companion star). Also, an analysis of the *INTEGRAL* data would be of interest to check if the changes in the hard X-ray flux of MN44 are related to any particular orbital phase.

Alternatively, as suggested by Masetti et al. (2010), MN44 could be a HMXB, i.e. a binary system composed of a massive star and a compact object, either a neutron star or black hole (van den Heuvel & Heise 1972; Tutukov & Yungelson 1973). In these systems, the hard X-ray emission is generated because of accretion of the stellar wind material onto the compact object, while its variability could be due to changeable accretion rate. In the case of MN44 the accretion rate could vary because of changes in the wind velocity and mass-loss rate of the LBV companion star and/or because of the eccentricity of the binary orbit. If the HMXB nature of MN44 would be confirmed (e.g. by detection of pulsed X-ray emission), then this system would represent a first known example of a HMXB with a bona fide LBV donor star (cf. Mason et al. 2012; Clark et al. 2013).

4.5 MN44: a runaway star?

MN44, like the majority of other bona fide and cLBVs, is located in the field and, therefore, is most probably a runaway star (Gvaramadze et al. 2012a,b). The runaway status of MN44 is also suggested by separation of this star from the Galactic plane (see Sect. 4.3). To check this possibility, we searched for proper motion measurements for MN44 using the Vizier catalogue access tool². We found four catalogues that provide proper motions for MN44, namely, UCAC2 (Zacharias et al. 2004), PPMXL (Röser, Demleitner & Schilbach 2010), SPM 4.0 (Girard et al. 2011) and UCAC4 (Zacharias et al. 2013). Since the measurement uncertainties in the first two catalogues are larger than the measurements themselves, we will use only the later two catalogues, which give $\mu_\alpha \cos \delta = -7.86 \pm 2.25$, $\mu_\delta = -2.59 \pm 2.41$ and $\mu_\alpha \cos \delta = -7.5 \pm 3.0$, $\mu_\delta = -5.6 \pm 3.0$, respectively.

Using the same Galactic constants and the solar peculiar motion as in Section 4.3, we calculated the peculiar transverse velocity of MN44, $v_{tr} = (v_l^2 + v_b^2)^{1/2}$, where v_l and v_b are the velocity components in the Galactic coordinates. For the sake of illustration, we adopted two plausible distances: 5.5 and 10.8 kpc. For the error calculation, only the errors of the proper motion measurements were considered. The results are summarized in Table 6.

Taken at face value, the obtained peculiar velocities imply that MN44 is a runaway star moving towards the Galactic plane, i.e. in the “incorrect” direction (recall that MN44 is located below the Galactic plane). However, the large error margins of the velocity components allow the possibility that MN44 is moving away from the Galactic plane at 2σ

Table 6. Peculiar transverse velocity and its components (in Galactic coordinates) for two adopted proper motion measurements and distances.

Sources for proper motions	d kpc	v_l (km s^{-1})	v_b (km s^{-1})	v_{tr} (km s^{-1})
SPM 4.0	5.5	-67 ± 61	99 ± 61	120 ± 61
UCAC4	5.5	-118 ± 78	38 ± 78	124 ± 78
SPM 4.0	10.8	36 ± 120	198 ± 120	201 ± 120
UCAC4	10.8	-64 ± 154	79 ± 154	102 ± 154

and 1σ significance level for the SPM 4.0 and UCAC4 proper motion measurements, respectively. Note also that the derived v_{tr} differs from zero only at $\approx 2\sigma$ or lower significance. Thus, to unambiguously prove the runaway status of MN44, one needs more precise proper motion measurements, which could be achieved with the space astrometry mission Gaia.

5 SUMMARY AND CONCLUSION

In this paper, we reported the discovery of a new (seventeenth) Galactic bona fide LBV. The discovery was made through the detection of a circular mid-infrared shell (of diameter of ≈ 30 arcsec) with the *Spitzer Space Telescope* and follow-up spectroscopic and photometric observations of its central star – MN44. The first epoch (2009) optical spectroscopy of MN44 revealed a rich emission spectrum, typical of LBVs near the visual maximum. The spectra taken six yr later showed the emergence of He I emission lines, which indicates that the star became hotter ($T_{\text{eff}} \approx 12\,000$ K). Besides, the EWs of the Balmer lines increased by ≈ 3 – 9 times, while the forbidden lines of [N II] and [Fe II], and some Fe II lines became much more prominent. Using the flat-topped [Fe II] $\lambda 5376$ line, we derived the terminal wind velocity of MN44 of $\approx 170 \text{ km s}^{-1}$ during the current hot state of this star, which could be considered as an indication that MN44 is close to its Eddington limit.

Our photometric observations showed that the spectral variability of MN44 is accompanied by the brightness decrease (~ 2 mag during the last six yr), which is typical of LBVs recovering from SDor-type outbursts. From archival photometric data, we also derived that MN44 has brightened in the I_c band by ≈ 3 mag in ≈ 30 yr preceding our observations. The large amplitude of photometric variability and the separation of MN44 from the Galactic plane were used to suggest that this star is located in the Norma arm, i.e. at ~ 5.5 or 10.8 kpc. At these distances, MN44 lies, respectively, ≈ 110 and 220 pc below the Galactic plane, which implies that MN44 is a runaway star.

Comparison of the *Spitzer* and SHS images revealed a knot of $\text{H}\alpha + [\text{N II}]$ emission to the northwest of MN44. The knot partially delineates the mid-infrared circumstellar shell, which is brighter in the place of possible contact with the knot. We suggested that the shell is interacting with a density inhomogeneity (knot) in the ambient medium. This suggestion was reinforced by the detection of enhanced nitrogen abundance in the knot, which might be caused by pollution from CNO-processed ejecta from MN44. Us-

² <http://webviz.u-strasbg.fr/viz-bin/VizieR>

ing the Balmer decrement in the spectrum of the knot, we derived the *V*-band extinction towards MN44 of 4.43 mag. This value turns out to be smaller by ≈ 6 mag than the extinction derived from dereddening the spectral slope of MN44. Two possible explanations of this discrepancy were discussed. The first one (our preference) is that MN44 is shrouded by dusty circumstellar material, which is responsible for most of the reddening of the star. Alternatively, the intrinsic Balmer decrement in the spectrum of the knot might be much shallower than what follows from the Case B recombination model. This could happen if the number density of the knot is $\gtrsim 10^{13} \text{ cm}^{-3}$.

We discussed possible association of MN44 with the *INTEGRAL* transient source of hard X-ray emission IGR J16327–4940. If real, this association would imply that MN44 is either a colliding-wind binary (similar to η Car and several other Galactic (c)LBVs) or a first known example of a HMXB with a bona fide LBV donor star.

To conclude, further spectroscopic and photometric monitoring of MN44 with better resolution and cadence would be of great importance for understanding the driving mechanisms of variability of this star, and, potentially, for revealing its duplicity. If the binary status of MN44 will be proved, then dedicated X-ray observations of this system would be highly desirable to search for orbital modulation of its X-ray flux (if the system is a wind-colliding binary) or X-ray pulsations from the compact object (if MN44 is a HMXB).

6 ACKNOWLEDGEMENTS

We are grateful to R.M.Humphreys (the referee) for useful comments and suggestions on the manuscript. Some observations reported in this paper were obtained with the Southern African Large Telescope (SALT). VVG and LNB acknowledge the Russian Science Foundation grants 14-12-01096 and 14-22-00041, respectively. AYK acknowledges support from the National Research Foundation (NRF) of South Africa. We thank Dave Kilkenny for getting for us *V*- and *I_c*-band images of MN44 with the SAAO 1-m telescope. This work is based in part on archival data obtained with the *Spitzer* Space Telescope, which is operated by the Jet Propulsion Laboratory, California Institute of Technology under a contract with NASA, and has made use of the NASA/IPAC Infrared Science Archive, which is operated by the Jet Propulsion Laboratory, California Institute of Technology, under contract with the National Aeronautics and Space Administration, the SIMBAD database and the VizieR catalogue access tool, both operated at CDS, Strasbourg, France.

REFERENCES

Asplund M., Grevesse N., Sauval A. J., Scott P., 2009, *ARA&A*, 47, 481
 Benjamin R. A. et al., 2003, *PASP*, 115, 953
 Benvenuti P., D’Odorico S., Peimbert M., 1973, *A&A*, 28, 447
 Berdnikov L. et al., 2012, *Astronomy Reports*, 56, 290
 Bird A. J. et al., 2010, *ApJS*, 186, 1

Buckley D. A. H., Swart G. P., Meiring J. G., 2006, in Stepp L. M., ed., *Proc. SPIE Conf. Ser. Vol. 6267, Ground-based and Airborne Telescopes*. SPIE, Bellingham, p. 62670Z
 Burgh E. B., Nordsieck K. H., Kobulnicky H. A., Williams T. B., ODonoghue D., Smith M. P., Percival J. W., 2003, in Iye M., Moorwood A. F. M., eds, *Proc. SPIE Conf. Ser. Vol. 4841, Instrument Design and Performance for Optical/Infrared Ground-based Telescopes*. SPIE, Bellingham, p. 1463
 Carey S. J. et al., 2009, *PASP*, 121, 76
 Clark J. S., Larionov V. M., Arkharov A., 2005, *A&A*, 435, 239
 Clark J. S., Crowther P. A., Larionov V. M., Steele I. A., Ritchie B. W., Arkharov A. A., 2009, *A&A*, 507, 1555
 Clark J. S., Bartlett E. S., Coe M. J., Dorda R., Haberl F., Lamb J. B., Negueruela I., Udalski A., 2013, *A&A*, 560, A10
 Conti P. S., 1984, in Maeder A., Renzini A., eds, *Observational Tests of the Stellar Evolution Theory*. Reidel, Dordrecht, p. 233
 Cordes J. M., Lazio T. J. W., 2002, *astro-ph/0207156*
 Crawford S. M. et al., 2010, in Silva D. R., Peck A. B., Soifer B. T., *Proc. SPIE Conf. Ser. Vol. 7737, Observatory Operations: Strategies, Processes, and Systems III*. SPIE, Bellingham, p. 773725
 Crowther P. A., Hillier D. J., Smith L. J., 1995, *A&A*, 293, 172
 Davidson K. et al., 1999, *AJ*, 118, 1777
 Drake S. A., Ulrich R. K., 1980, *ApJS*, 42, 351
 Fazio G. G. et al., 2004, *ApJS*, 154, 10
 Feldmeier A., Puls J., Pauldrach A. W. A., 1997, *A&A*, 322, 878
 Flagey N., Noriega-Crespo A., Petric A. O., Geballe T. R., 2014, *AJ*, 148, 34
 Georgelin Y. M., Georgelin Y. P., 1976, *A&A*, 49, 57
 Girard T. M. et al., 2011, *AJ*, 142, 15
 Groh J. H. et al., 2009, *ApJ*, 705, L25
 Gvaramadze V. V., Gualandris A., 2011, *MNRAS*, 410, 304
 Gvaramadze V. V., Kniazev A. Y., Fabrika S., 2010a, *MNRAS*, 405, 1047
 Gvaramadze V. V., Kniazev A. Y., Fabrika S., Sholukhova O., Berdnikov L. N., Cherepashchuk A. M., Zharova A. V., 2010b, *MNRAS*, 405, 520
 Gvaramadze V. V. et al., 2012a, *MNRAS*, 421, 3325
 Gvaramadze V. V., Weidner C., Kroupa P., Pflamm-Altenburg J., 2012b, *MNRAS*, 424, 3037
 Gvaramadze V. V., Kniazev A. Y., Berdnikov L. N., Langer N., Grebel E. K., Bestenlehner J. M., 2014, *MNRAS*, 445, L84
 Hamaguchi K. et al., 2014, *ApJ*, 795, 119
 Humphreys R. M., Davidson K., 1979, *ApJ*, 232, 409
 Humphreys R. M., Davidson K., 1994, *PASP*, 106, 1025
 Humphreys R. M., Davidson K., Smith N., 1999, *PASP*, 111, 1124
 Humphreys R. M., Weis K., Davidson K., Bomans D. J., Burggraf B., 2014a, *ApJ*, 790, 48
 Humphreys R. M., Davidson K., Gordon M. S., Weis K., Burggraf B., Bomans D. J., Martin J. C., 2014b, *ApJ*, 782, L21
 Keenan P. C., Hynek J. A., 1950, *ApJ*, 111, 1
 Kniazev A. Y., Gvaramadze V. V., Berdnikov L. N., 2015, *MNRAS*, 449, L60

- Kniazev A. Y., Pustilnik S. A., Grebel E. K., Lee H., Pramskij A. G., 2004, *ApJS*, 153, 429
- Kniazev A. Y. et al., 2005, *AJ*, 130, 1558
- Kniazev A. Y. et al., 2008, *MNRAS*, 388, 1667
- Kobulnicky H. A., Nordsieck K. H., Burgh E. B., Smith M. P., Percival J. W., Williams T. B., O'Donoghue D., 2003, in Iye M., Moorwood A. F. M., eds, *Proc. SPIE Conf. Ser. Vol. 4841, Instrument Design and Performance for Optical/Infrared Ground-based Telescopes*. SPIE, Bellingham, p. 1634
- Krueger T.K., Aller L.H., Czyzak S.J., 1970, *ApJ*, 160, 921
- Leyder J.-C., Walter R., Rauw G., 2008, *A&A*, 477, L29
- Masetti N. et al., 2010, *A&A*, 519, A96
- Mason A. B., Clark J. S., Norton A. J., Crowther P. A., Tauris T. M., Langer N., Negueruela I., Roche P., 2012, *MNRAS*, 422, 199
- Merrill P. W., 1934, *ApJ*, 79, 183
- Monet D. G. et al., 2003, *AJ*, 125, 984
- Nazé Y., Rauw G., Hutsemékers D., 2012, *A&A*, 538, A47
- Nazé Y., Corcoran M. F., Koenigsberger G., Moffat A. F. J., 2007, *ApJ*, 658, L25
- O'Donoghue D. et al., 2006, *MNRAS*, 372, 151
- Osmer P. S., 1972, *ApJS*, 24, 247
- Owocki S. P., Castor J. I., Rybicki G. B., 1988, *ApJ*, 335, 914
- Pallavicini R., Golub L., Rosner R., Vaiana G. S., Ayres T., Linsky J.L., 1981, *ApJ*, 248, 279
- Parker Q. A. et al., 2005, *MNRAS*, 362, 689
- Pickles A. J., 1998, *PASP*, 110, 863
- Reed B. C., 2000, *AJ*, 120, 314
- Reid M. J., Menten K. M., Zheng X. W., Brunthaler A., Xu Y., 2009, *ApJ*, 705, 1548
- Rieke G. H. et al., 2004, *ApJS*, 154, 25
- Röser S., Demleitner M., Schilbach E., 2010, *AJ*, 139, 2440
- Sana H., Rauw G., Nazé Y., Gosset E., Vreux, J.-M., 2006, *MNRAS*, 372, 661
- Saraph H.E., Seaton M.J., 1970, *MNRAS*, 148, 367
- Schönrich R., Binney J., Dehnen W., 2010, *MNRAS*, 403, 1829
- Skrutskie M. F. et al., 2006, *AJ*, 131, 1163
- Stahl O., Mandel H., Szeifert Th., Wolf B., Zhao F., 1991, *A&A*, 244, 467
- Stahl O. et al., 2001, *A&A*, 375, 54
- Stevens I. R., Blondin J. M., Pollock A. M. T., 1992, *ApJ*, 386, 265
- Stone R. C., 1979, *ApJ*, 232, 520
- Stringfellow G. S., Gvaramadze V. V., Beletsky Y., Kniazev A. Y., 2012a, in Richards M. T., Hubeny I., eds, *Proc. IAU Symp. 282, From Interacting Binaries to Exoplanets: Essential Modeling Tools*. Cambridge Univ. Press, Cambridge, p. 267
- Stringfellow G. S., Gvaramadze V. V., Beletsky Y., Kniazev A. Y., 2012b, in Drissen L., St-Louis N., Robert C., Moffat A. F. J., eds, *ASP Conf. Ser. Vol. 465, Four Decades of Massive Star Research – A Scientific Meeting in Honor of Anthony J. Moffat*. Astron. Soc. Pac., San Francisco, p. 514
- Tarter C. B., 1969, *ApJS* 18, 1
- The DENIS Consortium, 2005, *VizieR Online Data Catalog*, 2263, 0
- Tutukov A., Yungelson L. R., 1973, *Nauchn. Inform.*, 27, 86
- Usov V. V., 1992, *ApJ*, 389, 635
- van den Heuvel E. P. J., Heise J., 1972, *Nature Phys. Sci.*, 239, 67
- van Genderen A. M., de Groot M. J. H., The P. S., 1994, *A&A*, 283, 89
- Vega E. I., Rabolli M., Feinstein A., Muzzio J. C., 1980, *AJ*, 85, 1207
- Wachter S., Mauerhan J. C., van Dyk S. D., Hoard D. W., Kafka S., Morris P. W., 2010, *AJ*, 139, 2330
- Wachter S., Mauerhan J., van Dyk S., Hoard D. W., Morris P., 2011, *Bull. Soc. R. Sci. Liège*, 80, 291
- Wolf B., 1989, *A&A*, 217, 87
- Zacharias N., Urban S. E., Zacharias M. I., Wycoff G. L., Hall D. M., Monet D. G., Rafferty T. J., 2004, *AJ*, 127, 3043
- Zacharias N., Finch C.T., Girard T.M., Henden A., Bartlett J.L., Monet D.G., Zacharias M.I., 2013, *AJ*, 145, 44